

The Research on Full-speed Field Weakening Control Method of Electric Vehicle Interior Permanent Magnet Synchronous Motor

Run-Ze GAO^{1,a}, Li ZHAI² and Li-Wei SU³

¹From Research Institute of Highway Ministry of Transport (Beijing, 100088);

²From School of Mechanical Engineering, Beijing Institute of Technology (Beijing, 100081);

³From FAW-Volkswagen Automotive Co. Ltd. (Changchun, 130011)

Abstract. The motor drive system represents a key technology for development of the electrical vehicles, and the permanent magnet synchronous motor becomes the mainstream of the new energy vehicle drive motor for the superior performances in power density, low-speed torque density, efficiency and reliability. The paper studies the field weakening control strategy for the interior permanent magnet synchronous motor (IPMSM) and provides a field weakening control strategy for the IPMSM at the full-speed range. By studying the mathematical IPMSM model and the methods of conventional vector control and analyzing the operating conditions of the IPMSM at the full-speed range, the paper divides the operating conditions into constant torque operation region I, constant torque operation region II, constant power field weakening operation region and high-speed field weakening operation region to confirm the control strategy algorithm in each region and the transition conditions between regions and provide the current control strategy that the d-axis current and q-axis current are confirmed by the reference torque and the feedback speed. Modeling of the field weakening control strategies in each region is made through the Matlab/Simulink, and simulation of the operating conditions with a steady-state load and a dynamic load is done to verify that the field weakening control strategy in each region is feasible. A co-simulation is made by combining the Matlab/Simulink-based control model, the RecurDyn-based virtual prototype and the RT-LAB to verify the feasible field weakening control strategy.

Introduction

The PMSM features a small size, the low inertia and the fast response to have the superior performances in power density, low-speed torque density, efficiency and reliability. The motor of the kind is very adaptive to the electric vehicle's drive system to become the mainstream motor for the new energy vehicles at moment. The PMSM is subject to the common strategies for variable voltage and frequency control, field-orientated control and direct torque control.

To ensure the fast, accurate and precise system, the vector control theory has been extensively applied in the PMSM control system design for years. As the PMSM has the permanent magnetic (p-m) rotor with the approximately constant flux, it is controlled by means of the rotor flux orientation

^a Corresponding author: rz.gao@rioh.cn

in general. However, the field weakening expansion represents a key problem to hinder extensive application of the high-speed PMSM. For a decade, the domestic and foreign scholars have been attaching most importance to the problem and made great efforts to have a lot of study achievements. Unfortunately, these studies have the deficiencies in either the motor body or the control to combine speed, power and torque well. For this reason, the paper studies the field weakening strategy for the IPMSM to provide a field weakening strategy for the PMSM at the full-speed range.

1 Mathematical PMSM model

During analysis of the mathematical PMSM model, the following hypotheses are proposed to simplify the analysis process: The stator's armature winding generates a sine wave to induce the electromotive force and the rotor's permanent magnet also distributes the field of the sine wave form in the air-gap space; The eddy current and hysteresis losses are negligible for the core; The stator core has the negligible saturation with the constant inductance parameters and the magnetic circuit is considered linear; The damper winding is negligible for the rotor.

Based on the rotatory two-phase coordinates, the PM's fundamental wave exciter field axis is taken as the d axis and is rotated anticlockwise to surpass the d axis by 90° to take the electrical angle as the q axis. Both the d axis and the q axis are rotated at the rate of the electrical angle to determine the spatial coordinates with the electrical angle θ_r which is formed between the d axis and the reference axis A. The space sector of the PMSM in the coordinates is shown in Figure.1 below:

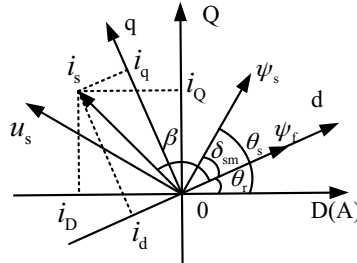


Figure. 1 PMSM Coordinate Sector Diagram

Where: The components of the d axis and the q axis may be obtained by shifting the three-phase stator winding in the coordinates (i.e. shift of the three-phase ABC coordinates to the rotatory dq coordinates).

$$\begin{cases} u_d = \frac{d\psi_d}{dt} - \omega_e \psi_q + R_s i_d \\ u_q = \frac{d\psi_q}{dt} + \omega_e \psi_d + R_s i_q \end{cases} \tag{1}$$

Where:

- u_d and u_q —Stator Voltage Components at the d axis and the q axis (V);
- ψ_d and ψ_q —Stator Flux-linkage Components at the d axis and the q axis (Wb);
- i_d and i_q —Stator Current Components at the d axis and the q axis (A);
- ω_e —Rotor's Electrical Angle (rad/s)

Flux-linkage Equation:

$$\begin{cases} \psi_d = L_d i_d + \psi_f \\ \psi_q = L_q i_q \end{cases} \tag{2}$$

$$\psi_s = \sqrt{\psi_d^2 + \psi_q^2} = \sqrt{(L_d i_d + \psi_f)^2 + (L_q i_q)^2} \quad (3)$$

Where:

ψ_s —Stator Flux-linkage (Wb);

L_d and L_q —Stator Winding Induction at the d axis and the q axis (H).

Back Electromotive Force Equation:

$$E_s = \omega_e \psi_s \quad (4)$$

Where:

E_s —Stator's Back Electromotive Force (V).

Torque Equation:

$$T_e = K p_n \psi_s \times i_s \quad (5)$$

Where:

T_e —Motor's Electromagnetic Torque (Nm);

K —Undetermined Coefficient;

i_s —Stator Current (A);

p_n —Pole Pairs of the Motor's Rotor.

In the paper, the torque is shown as follows:

$$\begin{aligned} T_e &= \frac{3}{2} p_n (\psi_s i_d - \psi_q i_q) \\ &= \frac{3}{2} p_n [\psi_f i_d + (L_d - L_q) i_d i_q] \end{aligned} \quad (6)$$

During the high-speed operation of the motor, the resistance's caused voltage loss is very little and negligible, so the equation (1) may be changed into:

$$\begin{cases} u_d = -\omega_e L_q i_q \\ u_q = \omega_e (L_d i_d + \psi_f) \end{cases} \quad (7)$$

For the IPMSM with the $L_d \neq L_q$, it is possible to control both the torque and the flux-linkage of the motor by controlling the quadrature-axis current and the direct-axis current respectively to improve the torque output capacity with the effective structural torque and change the flux-linkage for the field weakening control by controlling the direct-axis current.

2 Field weakening control algorithm

Restricted to the inverter output voltage and the motor current, the motor is limited to vary in current and terminal voltage in a specified scope and the stator current is limited by both the current limit circle and the voltage limit ellipse at the same time. i.e.:

$$\begin{cases} \sqrt{i_d^2 + i_q^2} = |i_s| \leq |i_s|_{\max} \\ \sqrt{u_d^2 + u_q^2} = |u_s| \leq |u_s|_{\max} \end{cases} \quad (8)$$

Where: i_s means the stator current sector and u_s means the stator voltage sector.

Combination of the equation (7) with the equation (8) may be simplified to obtain the current and voltage limit equations at the dq coordinates when the IPMSM is operating in a high-speed and stable state:

$$\begin{cases} \sqrt{i_d^2 + i_q^2} \leq |i_s|_{\max} \\ \left(\psi_f + L_d i_d \right)^2 + \left(L_q i_q \right)^2 \leq \left(\frac{|u_s|_{\max}}{\omega_e} \right)^2 \end{cases} \quad (9)$$

It is learned from the equation (9) that the current limit equation shows the circle (Dot: (0,0); Radius: $|i_s|_{\max}$) and the voltage limit equation shows the ellipse cluster whose center is located at the position of $(-\psi_f/L_d, 0)$ and the lengths of the semimajor axis and the semiminor axis are inversely proportional to the rotor's angular speed ω_e . Both the current limit circle and the voltage limit ellipse cluster at the dq coordinates are shown in Figure.2. In the event of $-\psi_f/L_d < i_{smax}$, the center of the voltage limit ellipse cluster exists outside of the current limit circle (see Figure. 2(a)); In the event of $-\psi_f/L_d > i_{smax}$, the center of the voltage limit ellipse cluster exists in the current limit circle (see Figure. 2(c)); Therefore, any intersection exists in the areas represented by the current limit circle and the voltage limit ellipse at any rotary speed. But no point of intersection will exist in the areas represented by the current limit circle and the voltage limit ellipse at an excessive rotary speed. In this case, the rotary speed is deemed possibly maximum for the motor in theory.

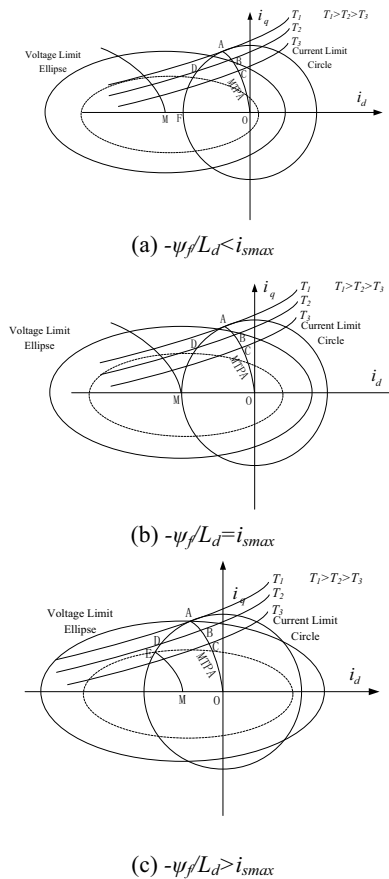


Figure. 2 Diagram of current and voltage sector for the PMSM operating at the full-speed range

3 Full-speed and Field Weakening Control Strategy

The maximum torque/current ratio curve of the IPMSM is shown by OA in the Figure. 2. Just take for example the torque T2 as given in Figure. 2(c), in the event of a given expected torque T2, the stator current sector remains unchanged as OB and the voltage sector increases at a higher rotatory speed of the motor, but when the voltage sector reaches the inverter's maximum output voltage $u_{s \max}$, it will fail to remain unchanged as OB and the motor will enter the constant torque region II. In this case, the appropriate rotatory speed of the motor may be defined as the turning speed from the constant torque region I to the constant torque region II to calculate A in the voltage limit ellipse equation (10). The Figure. 2 shows the greater the given expected torque, the lower the motor's turning speed from from the constant torque region I to the constant torque region II. The possible torque of the PMSM is indicated by the point A in the Figure. 2 to have the maximum stator current. Both the quadrature-axis current and the direct-axis current are shown in the equation (11) at the maximum torque.

$$\omega_A = \frac{u_{s \max}}{\sqrt{(L_d i_d + \psi_f)^2 + (L_q i_q)^2}} \quad (10)$$

$$\begin{cases} i_d = \frac{-\psi_f + \sqrt{\psi_f^2 + 8(L_d - L_q)^2 i_{s \max}^2}}{4(L_d - L_q)} \\ i_q = \sqrt{i_{s \max}^2 - i_d^2} \end{cases} \quad (11)$$

3.1 Gradient descent-based field weakening operation in the constant torque region II

When the motor operates in the constant torque region II, the voltage sector will continue the inverter's maximum output voltage and the stator current sector will increase at a higher rotatory speed. According to the Figure. 2(c), the constant torque curve and the maximum input power curve have the point of intersection in or outside of the current limit circle, depending upon the variation in the given expected torque. When the constant torque curve and the maximum input power curve have the point of intersection in the current limit circle, the motor will transit directly from the constant torque region II to the maximum input power operation region bypassing the ordinary constant torque field weakening operation region at a higher rotatory speed. In this case, the turning speed ω_D may be determined through the voltage limit ellipse where the constant torque curve and the maximum input power curve have the point of intersection. When the constant torque curve and the maximum input power curve have the point of intersection outside of the current limit circle, the motor will transit to the ordinary constant torque field weakening operation region first at a higher rotatory speed. In this case, the turning speed ω_B may be determined through the voltage limit ellipse where the constant torque curve and the current limit circle have the point of intersection (see the equation (12)). In the event of the minimum rotatory speed of entry into the maximum input power operation region, the motor will transit to the maximum input power operation region.

$$\begin{cases} i_d^2 + i_q^2 = i_s^2 \max \\ \omega_B = \frac{u_s \max}{\sqrt{(L_d i_d + \psi_f)^2 + (L_q i_q)^2}} \\ T_e = \frac{3}{2} \cdot p_n \cdot [\psi_f + (L_d - L_q) i_d] i_q \end{cases} \quad (12)$$

3.2 Ordinary constant torque field weakening operation

The stator current sector increases at a higher rotary speed of the motor. When the stator current sector reaches the maximum current $i_s \max$, the ultimate voltage ellipse and the constant torque curve will have the point of intersection outside of the current limit circle and the motor will fail to continue the constant torque output. Under this circumstance, to ensure continuous increase of the motor's rotary speed, it is possible to control the current sector changes along the point of intersection between the current limit circle and the voltage limit ellipse.

In the event of $i_d \geq -\psi_f/L_d$,

$$\begin{cases} i_d = \frac{-\psi_f L_d + \sqrt{\psi_f^2 L_d^2 - (L_d^2 - L_q^2) [\psi_f^2 - (u_s \max / \omega_e)^2 + L_q^2 i_s^2 \max]}}{L_d - L_q} \\ i_q = \sqrt{i_s^2 \max - i_d^2} \end{cases} \quad (13)$$

In the event of $i_d < -\psi_f/L_d$,

$$\begin{cases} i_d = \frac{-\psi_f L_d + \sqrt{\psi_f^2 L_d^2 - (L_d^2 - L_q^2) [\psi_f^2 - (u_s \max / \omega_e)^2 + L_q^2 i_s^2 \max]}}{L_d - L_q} \\ i_q = \sqrt{i_s^2 \max - i_d^2} \end{cases} \quad (14)$$

In the event of $\psi_f/L_d < i_s \max$, the ordinary constant torque field weakening operation region is divided into $i_d \geq -\psi_f/L_d$ and $i_d < -\psi_f/L_d$, depending upon the different functions for determination of the quadrature-axis current and the direct-axis current. During the transition from the $i_d \geq -\psi_f/L_d$ region to the $i_d < -\psi_f/L_d$ region, the turning speed ω_E may be determined through the $i_d = -\psi_f/L_d$ and $i_q = \sqrt{i_s^2 \max - i_d^2}$ the voltage limit ellipse equation and its appropriate maximum torque T_{02} may be determined through the constant torque curve where the $i_d = -\psi_f/L_d$ curve and the current limit circle have the point of intersection. As shown in Figure. 3, the constant torque curve and the current limit circle have the point of intersection at the left or right side of the $i_d = -\psi_f/L_d$ curve for the different given expected torques. When the constant torque curve and the current limit circle have the point of intersection at the left side of the $i_d = -\psi_f/L_d$ curve, the equation (13) and the equation (14) may be applied simultaneously to solve the system of binary linear equations and obtain the stator current sector components at the quadrature axis and the direct axis respectively. When the constant torque curve and the current limit circle have the point of intersection at the right side of the $i_d = -\psi_f/L_d$ curve, the equation (13) and the torque equation (6) may be applied simultaneously to solve the system of binary linear equations and obtain the stator current sector components at the quadrature axis and the direct axis respectively. As mentioned above, when the motor operates in the ordinary constant torque field weakening region, the stator current sector will change along the current limit circle at a higher rotary speed of the motor, and in the event of the minimum rotary speed of entry into the maximum input power operation region, the motor will transit from the ordinary constant torque field weakening operation region to the maximum input power region and the turning speed may be determined

through the voltage limit ellipse where the current limit circle and the maximum input power curve have the point of intersection.

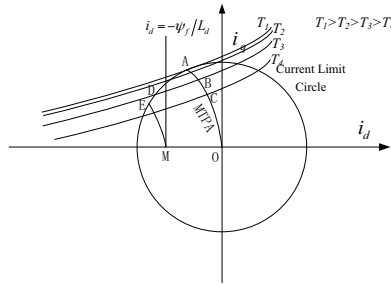


Figure. 3 Division of the ordinary constant torque field weakening region

3.3 High-speed and field weakening operation

The maximum input power control locus is shown in Figure. 2(c). The locus is intersected with the current limit circle at the point E which represents the minimum rotary speed C to provide the field weakening control at the maximum input power and may be determined through the voltage limit ellipse where the point E exists in the following equation (15). When the given expected torque is greater than the point A's appropriate maximum torque T01, the motor will bypass the constant torque field weakening region and enter the maximum input power operation region directly and the T01 may be determined through the constant torque curve where the point E exists in the equation (16). When the motor operates in the maximum input power region, the stator current sector will move along the maximum input power field weakening control locus toward the center point M of the voltage limit ellipse cluster. The point M has the coordinates of $(-\psi_f/L_d, 0)$ to show the ultimate operation. That is, the demagnetizing field of the direct-axis current is equivalent to the exciter field of the permanent magnet at the point to make the motor speed infinitely great in theory. The motor speed will increase along the curve until balance of the electromagnetic torque and the load torque.

$$\omega_c = (\rho - 1) \frac{\sqrt{2\rho + [3(\rho)^2 - 4\rho + 1]\sqrt{4k_{s,max}^2\rho^2 + 4k_{s,max}^2 + 4\rho - 3} + 4k_{s,max}^2 + 5\rho^2 - 6\rho^3 + 2\rho^4 + \rho^5 - 3}}{\rho\sqrt{2[4k_{s,max}^2 - 5k_{s,max}^2\rho^2 + 12k_{s,max}^2\rho - 7k_{s,max}^2 + \rho^3 - 6\rho^3 + 12\rho^2 - 10\rho + 3]}} \tag{15}$$

$$\begin{cases} i_d = -\frac{\psi_f}{L_d} + \Delta i_d \\ i_q = -\frac{\sqrt{(u_{s,max}/\omega_c)^2 - (L_d \Delta i_d)^2}}{L_q} \\ \Delta i_d = \left(\sqrt{L_q^2 \psi_f^2 + 8(L_d - L_q)^2 \left(\frac{u_{s,max}}{\omega_c}\right)^2} - L_q \psi_f \right) / \left[4L_d(L_d - L_q) \right] \\ i_d^2 + i_q^2 = i_{s,max}^2 \\ T_{01} = \frac{3}{2} \cdot p_n \cdot (\psi_f + (L_d - L_q) i_d) i_q \end{cases} \tag{16}$$

$$\begin{cases} T_e = \frac{3}{2} \cdot p_n \cdot (\psi_f + (L_d - L_q) i_d) i_q \\ i_d = -\frac{\psi_f}{L_d} + \Delta i_d \\ i_q = -\frac{\sqrt{(u_s \max / \omega_D)^2 - (L_d \Delta i_d)^2}}{L_q} \\ \Delta i_d = \left(\sqrt{L_q^2 \psi_f^2 + 8(L_d - L_q)^2 \left(\frac{u_s \max}{\omega_D} \right)^2} - L_q \psi_f \right) / \left[4L_d(L_d - L_q) \right] \end{cases} \quad (17)$$

4 Simulation results

4.1 Simulation comparison between the MTPA control and the id=0 control

It is assumed that the expected torque is $T_e=145\text{Nm}$ and the load torque $T_L=50\text{Nm}$, the waveform variation of the motor which is controlled through the MTPA and the $i_d=0$ is shown in Figure. 4~Figure. 9 in output torque, rotary speed, direct-axis current, stator current, stator voltage and flux-linkage.

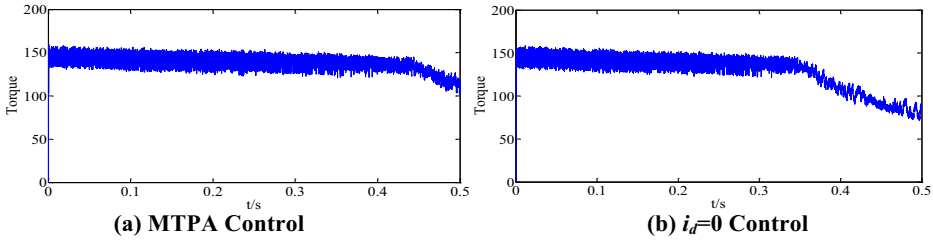


Figure. 4 Torque change curve

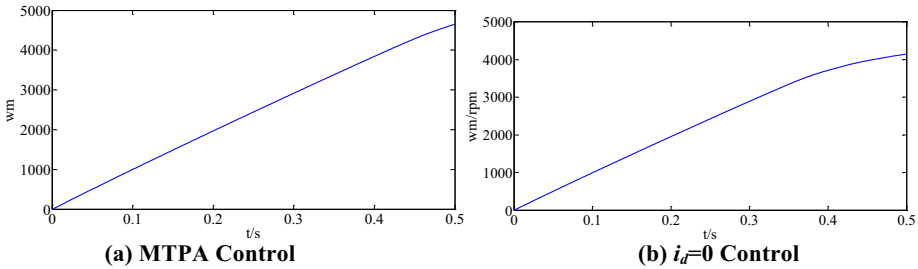


Figure. 5 Rotary speed change curve

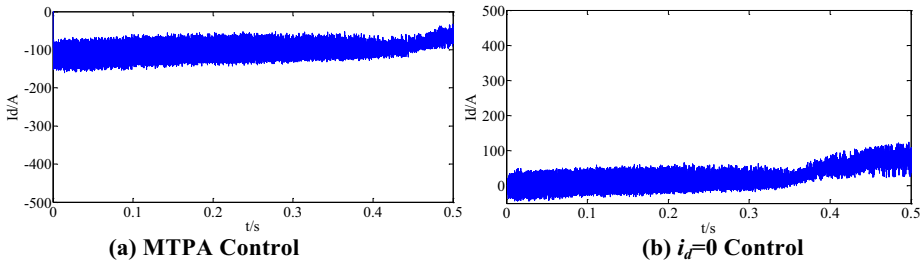


Figure. 6 Direct-axis current change curve

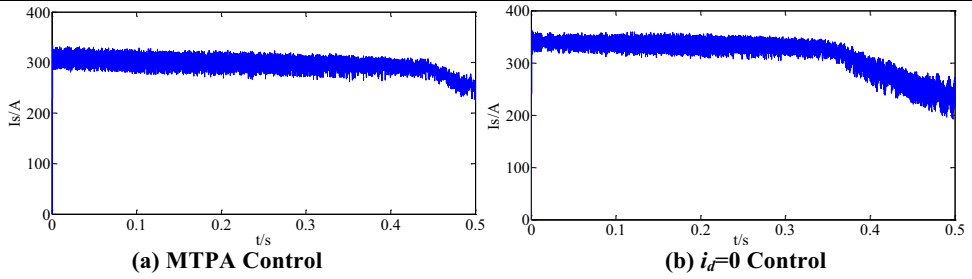


Figure. 7 Stator current change curve

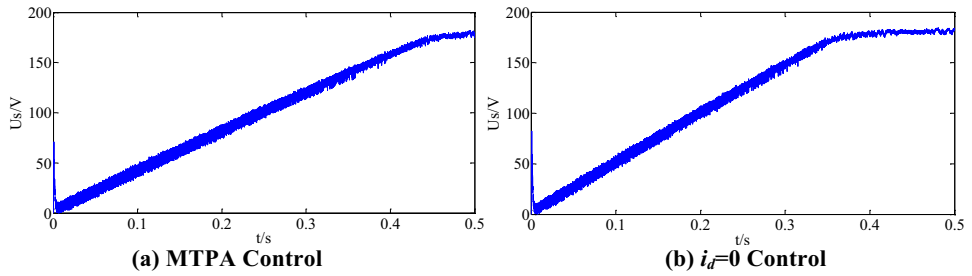


Figure. 8 Stator voltage change curve

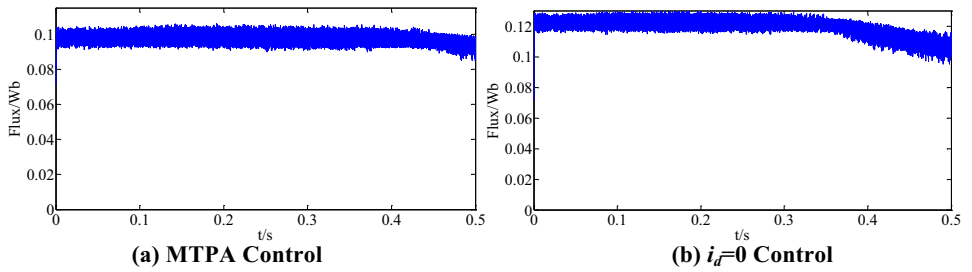


Figure. 9 Flux-linkage change curve

According to the Figure. 4, in the event of the MTPA control, the motor maintains the output torque of 145Nm or so for about 0.45s before the automatic field weakening link; In the event of the $i_d=0$ control, the motor's output torque maintains for about 0.35s before the drop. Therefore, the MTPA may provide the expected output torque for a longer period of time when a similar torque is expected. According to the Figure. 5, in the event of the MTPA control, the motor will have the rotary speed of up to 4,500rpm at 0.45s, while in the event of the $i_d=0$ control, it will have the speed of no more than 3,500rpm at 0.35s. Therefore, the MTPA control may provide a higher turning speed when a similar torque is expected. According to the Figure. 6, in the event of the MTPA control, the direct-axis current I_d will remain at the -100A or so with the existing reluctance torque. But in the event of the $i_d=0$ control, the direct-axis current I_d will be zero without the reluctance torque. According to the Figure. 7, in the event of the similar expected output torque T_e of 145Nm, the stator current of 300A is required for the MTPA control and the stator current of 350A for the $i_d=0$ control to show decrease of the current by 14.3%. Therefore, the MTPA control may improve the current utilization. The stator voltage change curve (see Figure. 8) indicates whether or not the stator has the maximum voltage to

identify if the stator enters the field weakening control phase. According to the Figure. 9, the stator has the flux-linkages of 0.1Wb and 0.12Wb for the MTPA control and the $i_d=0$ control respectively. Therefore, the MTPA is actually also the field weakening control, but the flux-linkage remains unchanged in the MTPA control phase (i.e. constant flux-linkage field weakening control).

4.2 Simulated field weakening control of the PMSM operating at the full-speed range

By applying the load force model in the field weakening control model for the PMSM, the expected torque of 100Nm is taken for the simulations as shown in Figure. 10~Figure. 15. Considering the selected expected torque of greater than T_J , the PMSM operates in one region after another (namely, the maximum torque/current ratio operation region, the constant torque region II, the ordinary constant power field weakening region and the maximum output power control region). The quadrature/direct-axis current, the stator current, the flux-linkage and the output torque remain unchanged in the constant value with the slow power increase at the beginning of the PMSM operation at the maximum torque/current ratio; At $t=0.5$ s, the direct-axis current begins to increase inversely and the PMSM transits from the maximum torque/current ratio operation region to the constant torque region II where the output torque remains constant with the continuous reverse increase of the direct-axis current and the stator current begins to increase from the constant value for the maximum torque/current ratio operation region with the continuous power increase; At $t=0.7$ s, the stator current becomes the highest; the PMSM transits from the constant torque region II to the ordinary constant torque field weakening region with the continued reverse increase of the direct-axis current; and the motor's output torque begins to drop with the absolute value of the direct-axis current remaining unchanged; At $t=1$ s, the PMSM transits from the ordinary constant torque field weakening region to the maximum output power control region with decrease of the direct-axis current in the absolute value, drop of the stator current and power from the constant values and continuous reduction of the output torque until the PMSM tends to have the stable operation when the output torque is equivalent to the load torque at $t=1.5$ s. According to the Figure. 12 and the Figure. 14, during the operation simulation, the motor has the continuous increase of the rotary speed to ensure the stability and balance, while the stator flux-linkage remains unchanged in the maximum torque/current ratio operation region and begins to decrease after entry into the constant torque region II until the motor has the stability and balance.

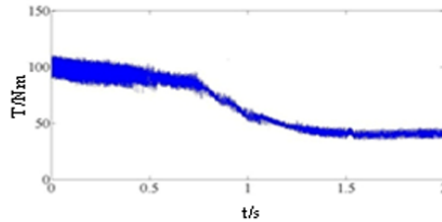


Figure. 10 Torque Change Curve

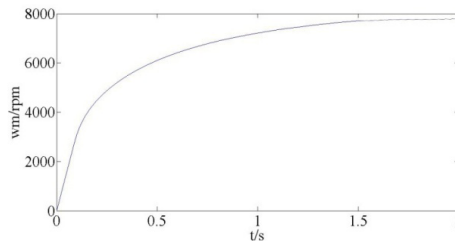


Figure. 11 Rotary Speed Change Curve

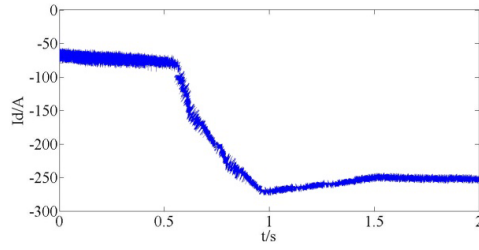


Figure. 12 Direct-axis Current Change Curve

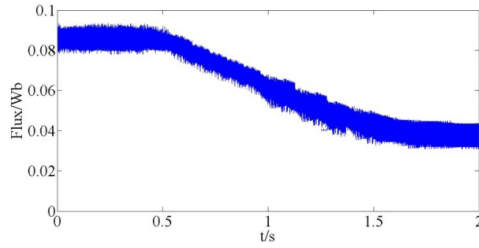


Figure. 13 Stator Flux-linkage Change Curve

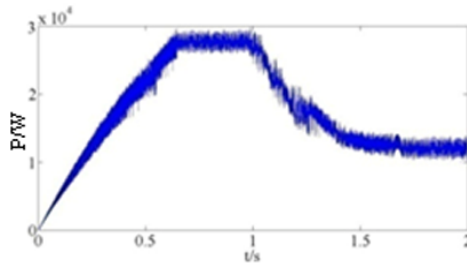


Figure. 14 Power Change Curve

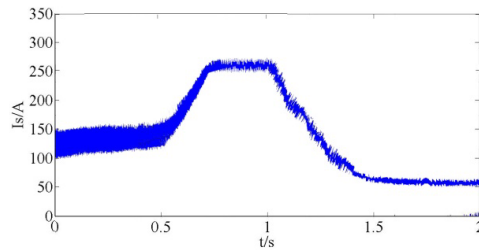


Figure. 15 Stator Current Change Curve

Conclusion

The paper studies the field weakening control strategy for the interior permanent magnet synchronous motor (IPMSM) and provides a field weakening control strategy for the IPMSM at the full-speed range. By studying the mathematical IPMSM model and the methods of conventional vector control and analyzing the operating conditions of the IPMSM at the full-speed range, the paper divides the operating conditions into constant torque operation region I, constant torque operation region II, constant power field weakening operation region and high-speed field weakening operation region to confirm the control strategy algorithm in each region and the transition conditions between regions and provide the current control strategy that the d-axis current and the q-axis current are confirmed by the reference torque and the feedback speed.

Acknowledgment

Funded by the National Natural Science Foundation of China (No.: 50975027).

References

1. Chen Qingquan, Sun Fengchun and Zhu Jianguang, *Modern Electric Vehicle Technology* [M]. Beijing: Beijing Institute of Technology Press, 2002.
2. Sun Xudong and Wang Shanming, *Electromechanics*[M]. Beijing: Tsinghua University Press, 2006.
3. Dai Ying, Wang Lixin and Cui Shumei. *Review of the Permanent Magnet Synchronous Motor for Electrical Vehicles*[J], *Micromotor*, 2005, 38(3):84-86.
4. Wang Xiuhe, *Permanent Magnet Motor* [M]. Beijing: China Electric Power Press.
5. Guo Qingding, Sun Yibiao and Wang Limei, *Modern PMSM & AC-Servo System*[M]. Beijing: China Electric Power Press, 2006.
6. Wu Anshun, *The Newest Practice Speed Control System for AC Motor*[M]. Beijing: China Machine Press, 1998.
7. Zong Shiyong, *Hybrid Electric Vehicle Permanent magnet Synchronous Motor Vector Control*[D]. Hunan University: Control Science and Engineering, 2010.
8. Xu Yanliang, *Study of the PMSM for Electric Vehicles in Power Characteristics and Field Weakening Speed Expansion Capability* [J]. *Transactions of China Electrotechnical Society*, 2004, 6:58-62.
9. W. L. Soong, D. A. Staton, and T. J. E. Miller, Design of a new axially laminated interior permanent magnet motor [J]. *IEEE Transactions on Industry Applications*, vol. 31, pp. 358-367, 1995.
10. C. Deak, A. Binder, B. Funieru, Extended field weakening and overloading of high-torque density permanent magnet motors[J], in 2009 Energy Conversion Congress and Exposition, pp. 2347-2353, 2009.
11. S. Bolognani, S. Bolognani, L. Peretti. Combined speed and current model predictive control with inherent field-weakening features for PMSM drives[J]. *IEEE Electrotechnical conference*, pp. 472-478, 2008.
12. Yasser Abdel-Rady Ibrahim Mohamed. Adaptive Self-Tuning MTPA Vector Controller for IPMSM Drive System[J]. *IEEE TRANSACTIONS ON ENERGY CONVERSION*, 2006, 3:636-644.
13. ZHAI Li, DONG Shou-quan, SU Li-wei. Optimal DTC Strategy of PMSM in Electric Vehicle[C]. *World Congress on Intelligent Control and Automation*, 2012.7.6. to be published.